Acoust. Sci. & Tech. **26**, 2 (2005)

PAPER

Numerical examination on scattering coefficients of architectural surfaces using the boundary element method

Yoshiyuki Kosaka* and Tetsuya Sakuma†

Institute of Environmental Studies, The University of Tokyo, Hongo 7–3–1, Bunkyo-ku, Tokyo, 113–8656 Japan

(*Received 5 July 2004, Accepted for publication 25 December 2004*)

Abstract: In order to evaluate the scattering coefficients of architectural surfaces, a numerical technique based on Mommertz's definition is developed with employing a 3-dimensional boundary element method. Numerical examination on the setting of parameters in computation and the conditions of samples is performed so as to ensure accurate calculation with this technique. As a result, criteria for the numerical parameters and for the test arrangement are clarified, and additionally, illustrating the behavior of directional and random-incidence scattering coefficients. Furthermore, in comparison between the values with the present method and those for an infinite periodic surface, general correspondence is confirmed although some differences appear due to the edge diffraction by the finite sample.

Keywords: Scattering coefficient, Specular reflection, Diffuser, Periodic surface, Numerical analysis, Boundary element method

PACS number: 43.20.Fn, 43.55.Br, 43.55.Ka [DOI: 10.1250/ast.26.136]

1. INTRODUCTION

There are many researches concerning sound scattering of surfaces, where several kinds of indices of scattering performance were proposed [1–5]. As one of the indices, the scattering coefficient is defined as the ratio of the non-specularly reflected acoustic energy to the totally reflected energy (see Fig. 1) [5], which is simply represented by

$$s(\theta', \varphi') = 1 - \frac{E_{\mathrm{spec}}}{E_{\mathrm{total}}}, \tag{1}$$

where E_{total} and E_{spec} are the total and the specularly reflected energy, respectively. It can be directly utilized to improve the accuracy of geometric room acoustic simulation, and furthermore, to compare the performance of diffusing surfaces in room acoustic designing. At the present, a method of measuring the random-incidence scattering coefficient is being standardized by ISO [6], however, unclear points on test arrangement and procedure still remain [7–9].

On the other hand, numerical evaluation of scattering coefficients is so powerful as to realize various parametric studies in an ideal sound field modeling. Mommertz [10] proposed alternative determination of scattering coefficients from the reflection directivity of surfaces in the free field, which is suitable for numerical modeling. Based on the determination, Embrechts *et al.* [11] theoretically analyzed random rough surfaces by using Kirchhoff approximation method, and Gomes *et al.* [12] calculated the coefficients under 45 degrees incidence by a 2-dimensional boundary element method.

In this paper, a numerical technique based on Mommertz's definition, with employing a 3-dimensional boundary element method, is presented for evaluating scattering performance of architectural surfaces with arbitrary shapes, as a substitute for ISO measurement. Consequently, numerical modeling is intended to be comparable with the sample arrangement in the ISO measurement method. To ensure the accuracy of this technique, appropriate criteria for the setting of computational parameters and the conditions of samples are clarified through numerical examination. Additionally, numerical results with this technique are compared with those for an infinite periodic surface.

2. NUMERICAL METHOD

2.1. Calculation of Scattering Coefficients

Consider that a plane wave impinges on a sample in the free field as shown in Fig. 2, where (θ', φ') and (θ, φ) are the incidence and the reflection angles, respectively. Here, the

*e-mail: kosaka@env.arch.t.u-tokyo.ac.jp
†e-mail: sakuma@k.u-tokyo.ac.jp

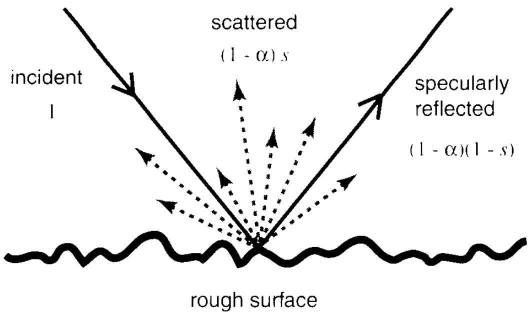

Fig. 1 Scattering from rough surface with an incident wave of unit-amplitude, where α is the absorption coefficient and s is the scattering coefficient.

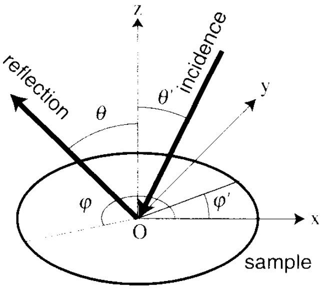

Fig. 2 Geometry of the numerical model.

directions in the upper hemisphere are sampled at constant intervals of polar and azimuthal angles as follows:

$$\Delta\theta_{ij} = \frac{\pi/2}{N_\theta}, \quad \theta_{ij} = \left(i - \tfrac{1}{2}\right)\Delta\theta_{ij}, \quad (i = 1, 2, \ldots, N_\theta),$$

$$\Delta\varphi_{ij} = \frac{\pi/2}{N_\varphi}, \quad \varphi_{ij} = \left(j - \tfrac{1}{2}\right)\Delta\varphi_{ij}, \quad (j = 1, 2, \ldots, 4N_\varphi),$$

where $N_\varphi = \lceil N_\theta \sin\theta_{ij} \rceil$.

Based on Mommertz's definition [10], the incidence-angle-dependent scattering coefficient is calculated from the two reflection directivities for the sample and for the flat reference plate with the same size, which is represented by

$$s(\theta', \varphi') = 1 - \frac{|R_{10}|^2}{R_{00} \cdot R_{11}}, \tag{2}$$

where $R_{xy} = \sum_{i=1}^{N_\theta} \sum_{j=1}^{4N_\varphi} p_x(\theta_{ij}, \varphi_{ij}) p_y^*(\theta_{ij}, \varphi_{ij}) \sin\theta_{ij} \Delta\theta_{ij} \Delta\varphi_{ij}$, p_1 and p_0 denote the complex sound pressure for the sample and for the reference, respectively, and $*$ indicates complex conjugate. Throughout this paper, surfaces are assumed to be perfectly reflective. Finally, according to Paris' formula [13], integrating the above directional values over the upper hemisphere gives the random-incidence scattering coefficient as follows

$$\bar{s} = \frac{1}{\pi} \sum_{i=1}^{N_\theta} \sum_{j=1}^{4N_\varphi} s(\theta'_{ij}, \varphi'_{ij}) \sin\theta'_{ij} \cos\theta'_{ij} \Delta\theta'_{ij} \Delta\varphi'_{ij}. \tag{3}$$

2.2. Calculation of Reflection Directivity with BEM

On the assumption that the sample and the reference plate have negligible thickness, applying the boundary element method in the normal derivative form on every incidence condition gives the following matrix equation

$$A_N \cdot \tilde{\boldsymbol{P}} = \boldsymbol{D}, \tag{4}$$

where $A_{N_{ij}} = \iint_{e_j} \frac{\partial^2 G(\boldsymbol{r}_i, \boldsymbol{r}_q)}{\partial n_i \partial n_q} dS_q$, $\tilde{\boldsymbol{P}} = [\tilde{\boldsymbol{p}}_1, \tilde{\boldsymbol{p}}_2, \ldots, \tilde{\boldsymbol{p}}_l, \ldots]$, $D_{il} = \frac{\partial}{\partial n_i} \exp(-j\boldsymbol{k}_l \cdot \boldsymbol{r}_i)$, e_j is the j-th element, $\boldsymbol{r}_i$ is the position vector of i-th node, $\boldsymbol{r}_q$ is the position vector of source point q in j-th element, $\partial/\partial \boldsymbol{n}$ denotes the normal derivative (outward direction is positive), $\boldsymbol{k}_l$ is the wave number vector for l-th incidence condition, and $\tilde{p}_{jl}$ (the j-th element of the vector $\tilde{\boldsymbol{p}}_l$) is the sound pressure difference on both surfaces of j-th element for l-th incidence condition. Consequently, the sound pressure differences for every incidence condition are simultaneously calculated by $\tilde{\boldsymbol{P}} = A_N^{-1} \cdot \boldsymbol{D}$.

Considering that the receiving point for every direction is far from the center of the sample at a certain distance, the reflected sound pressure distribution for every incidence condition can be calculated by the following equation,

$$\boldsymbol{P}^r = -\boldsymbol{A} \cdot \tilde{\boldsymbol{P}}, \tag{5}$$

where $\boldsymbol{P}^r = [\boldsymbol{p}_1^r, \boldsymbol{p}_2^r, \ldots, \boldsymbol{p}_l^r, \ldots]$, $A_{mj} = \iint_{e_j} \frac{\partial G(\boldsymbol{r}_m, \boldsymbol{r}_q)}{\partial n_q} dS_q$, and p_{ml}^r is the reflected sound pressure at m-th receiving point for l-th incidence condition. Once the reflection directivities for the sample and the reference plate are calculated in the above way, then the directional and the random-incidence scattering coefficients are obtained by Eqs. (2) and (3).

3. SETTING OF NUMERICAL PARAMETERS

In order to give appropriate setting of numerical parameters in the present method, this section investigates the influence of the parameters on the calculated results. In the following calculation, if there is no special mention, the boundary element analysis is performed using triangle constant elements with a width less than 1/5 of the wavelength, at 1/3 octave-band center frequencies, the distance from the center of the sample to receivers is infinity, and the directional parameter $N_\theta = 30$.

3.1. Location of Receiving Points

For determining reflection directivity, the distance from the center of the sample to the receiving points should be fixed at a certain value, so that the influence of the distance on the result is examined here. Figure 3 illustrates a test sample of the diameter of 3 m, with periodic sinusoidal surface. The surface period L is 0.2 m and the height h is 0.06 m. With changing the distance d, the random-incidence scattering coefficients are calculated by the method.

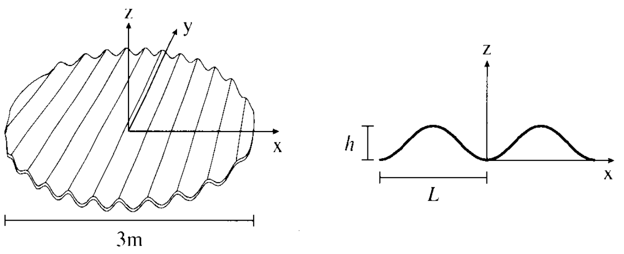

Fig. 3 Illustration of the sample with sinusoidal periods.

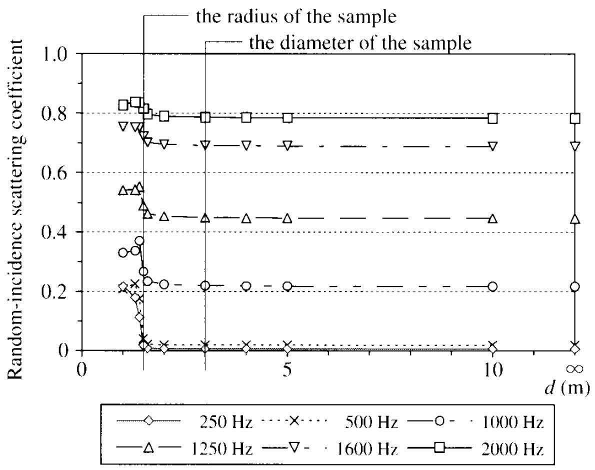

Fig. 4 Variation of the random-incidence scattering coefficients due to the receiver distance d.

Figure 4 shows the influence of the distance on the calculated coefficients. It is seen that large difference between the values for near and for far receiving points at lower frequencies, however, the coefficients sufficiently converge at certain values if the distance is more than the diameter of the sample. This finding is applicable for measurement setting, while it is consistent for numerical analysis to give the distance infinity.

3.2. Directional Discretization

As described in subsection 2.1, the method employs the directional discretization for incidence and reflection angles by means of the parameter N_θ. Changing the parameter as shown in Table 1, the influence of the directional discretization is examined with the same sample

Table 1 Conditions for directional discretization.

N_θ	Number of directions ($0^\circ \leq \theta, \varphi \leq 90^\circ$)	$\Delta\theta_{ij}$ (deg)
9	56	10
15	150	6
18	214	5
30	586	3
45	1,310	2

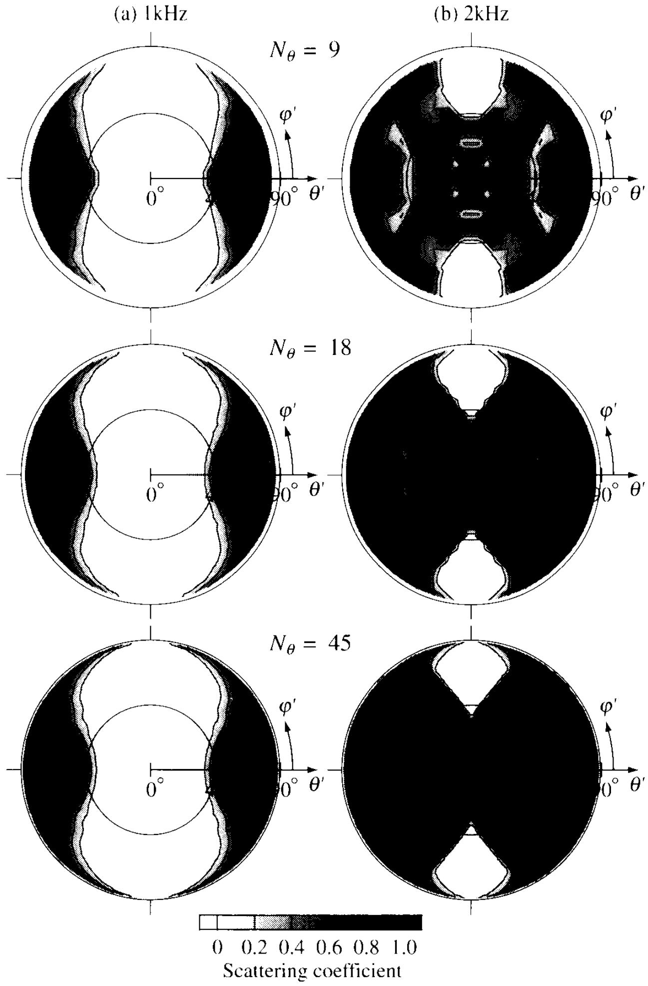

Fig. 5 Distribution of the directional scattering coefficients calculated with $N_\theta = 9$, 18 and 45: (a) 1 kHz and (b) 2 kHz.

as used in the previous study.

Figure 5 illustrates the distribution of the directional scattering coefficients calculated at 1 kHz and 2 kHz, on the three conditions that $N_\theta = 9$, 18 and 45. Very little difference among the results is seen at 1 kHz, however, the result with $N_\theta = 9$ is remarkably different from the other two at 2 kHz.

Figure 6 shows the random-incidence scattering coefficients calculated under every condition. Below 1 kHz, good agreement is seen among all conditions, while some difference gradually arises at higher frequencies. Figure 7 shows the differences ϵ_{dd} between the random-incidence values on the two conditions for directional discretization. Here, ϵ_{dd} is defined as

$$\epsilon_{dd} = \frac{|\bar{s}_1 - \bar{s}_2|}{|N_{\theta,1} - N_{\theta,2}|}. \tag{6}$$

It is seen that ϵ_{dd} between the results with $N_\theta = 18$ and 30 are smaller than 0.01 at all frequencies. Therefore, in the range up to 2 kHz, the condition $N_\theta = 18$ ($\Delta\theta_{ij} = 5^\circ$) is

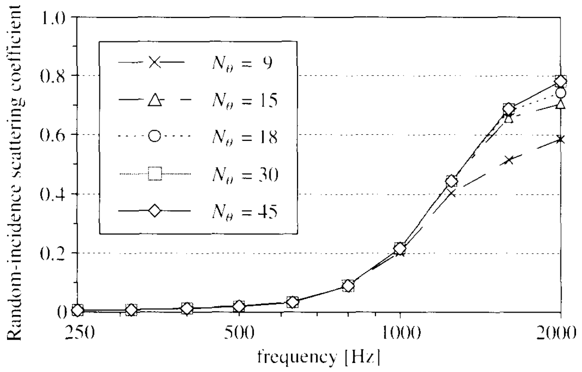

Fig. 6 Random-incidence scattering coefficients calculated with changing N_θ.

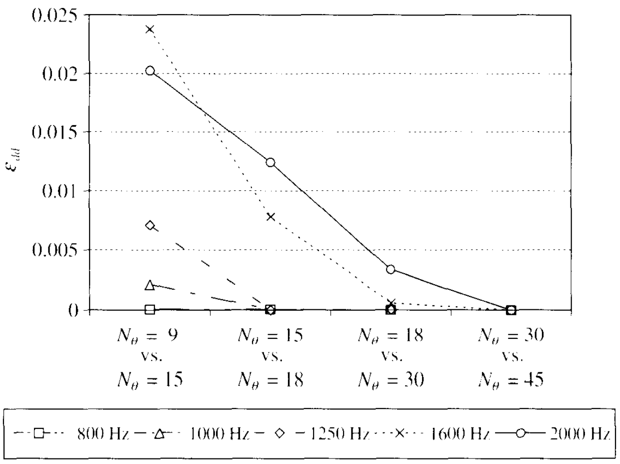

Fig. 7 Differences between the random-incidence values on the two conditions for directional discretization. ϵ_{dd} is defined as Eq. (6).

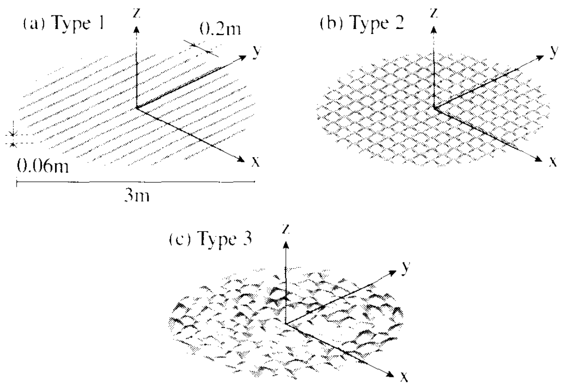

Fig. 8 Test samples: (a) 1D sinusoidal periods (Type 1), (b) 2D sinusoidal periods (Type 2), and (c) pseudo-random rough surface (Type 3).

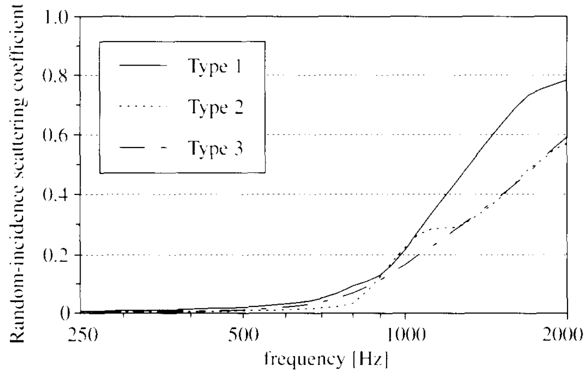

Fig. 9 Random-incidence scattering coefficients at 1/12 octave-band center frequencies for the three types of samples.

considered to be applicable, and the condition $N_\theta = 30$ ($\Delta\theta_{ij} = 3^\circ$) to be reliable. This result is roughly in accordance with the criterion $\Delta\theta \leq 50\lambda/D$ (deg) (λ is the wavelength and D is the dimension of the test sample, here, $D = 3$ m), which is for receiver sampling in calculation of polar patterns on a semicircle in a single plane, proposed by Embrechts *et al.* [11].

3.3. Frequency Intervals

In the previous studies, the results at 1/3 octave-band center frequencies were presented for the discussion. However, the detailed behavior of the random-incidence scattering coefficients in 1/3 octave-bands should be examined to give appropriate frequency intervals in the practical calculation of 1/3 octave-band values. Figure 8 illustrates three types of test samples with the same height (0.06 m): 1D sinusoidal surface (Type 1), 2D sinusoidal surface (Type 2), and pseudo-random rough surface (Type 3). The rms heights are 0.0367 m (Type 1), 0.0225 m (Type 2), and 0.0242 m (Type 3), respectively, and Type 3 is composed of pyramids (the density of summits is 21.93 m^{-2}).

Figure 9 shows the random-incidence scattering coefficients calculated at 1/12 octave-band center frequencies. Although moderate fluctuation appears in the case with Types 1 and 2, all lines are fairly smooth.

Subsequently, the averages of the above values in 1/3 octave-bands, and the values at 1/3 octave-band center frequencies are compared in Table 2. As a result, the difference between the averages of the values at 1/6 and 1/12 octave-band center frequencies is considered to be negligible in these cases. Additionally, the difference between the values at 1/3 octave-band center frequencies and the other averages is 0.025 at most. Therefore, it can be said that single frequency analysis at 1/3 octave-band center frequencies is practically useful for rough evaluation of scattering coefficients.

4. ARRANGEMENT OF TEST SAMPLES

In this section, two aspects of the arrangement of test samples are examined by numerical analysis, regarding the

Table 2 Random-incidence scattering coefficients of 1/3 octave-bands: (a) the values at the center frequencies, (b) the averages of the values at 1/6 octave-band center frequencies, and (c) the averages of the values at 1/12 octave-band center frequencies.

		315 Hz	400 Hz	500 Hz	630 Hz	800 Hz	1,000 Hz	1,250 Hz	1,600 Hz
Type 1	(a)	0.008	0.013	0.020	0.034	0.091	0.216	0.446	0.688
	(b)	0.009	0.013	0.020	0.036	0.090	0.226	0.446	0.667
	(c)	0.009	0.013	0.020	0.036	0.089	0.225	0.445	0.673
Type 2	(a)	0.003	0.005	0.008	0.012	0.033	0.225	0.291	0.435
	(b)	0.003	0.005	0.008	0.013	0.058	0.212	0.306	0.430
	(c)	0.003	0.005	0.008	0.013	0.054	0.216	0.304	0.433
Type 3	(a)	0.004	0.006	0.010	0.023	0.067	0.166	0.287	0.434
	(b)	0.004	0.006	0.011	0.025	0.073	0.170	0.288	0.433
	(c)	0.004	0.006	0.011	0.025	0.071	0.170	0.287	0.433

outlined shape of general samples and the number of periods for typical samples with periodic surface. Basically, the setting for numerical analysis is as used for the reference condition in the previous section.

4.1. Shape of Test Samples

In the ISO measurement method, test samples should have circular shape, because sample rotation is employed to extract the specularly reflected component by synchronized averaging of impulse responses. On the other hand, Mommertz's definition has in principle no restriction on the shape of samples. If square shape can be applied as well as circular shape, it is very useful for numerical analysis concerning mesh generation and calculation efficiency. Thus, in this subsection, two sets of samples with circular and square shape as illustrated in Fig. 10, are tested to investigate the influence of the shape. Here, the diameter is 3 m for circular samples, while the side length is 3 m for square ones, and quadrilateral constant elements with a width less than 1/5 of the wavelength are employed for Type 1s.

Figure 11 shows an example of calculated results, illustrating the distribution of the directional scattering coefficients at 1 kHz and 2 kHz for the circular and the square samples with 2D sinusoidal periods. The difference between them is quite small, and this tendency is seen at any frequencies regardless of the sample type.

As is also seen in Fig. 12, which illustrates the random-incidence values, it was confirmed that the influence of the shape of test samples is negligible in the present numerical method.

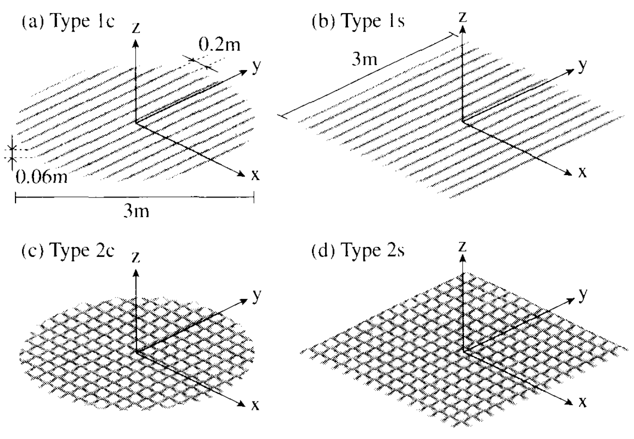

Fig. 10 Test samples: (a) circular with 1D sinusoidal periods (Type 1c), (b) square with 1D ones (Type 1s), (c) circular with 2D ones (Type 2c), and (d) square with 2D ones (Type 2s).

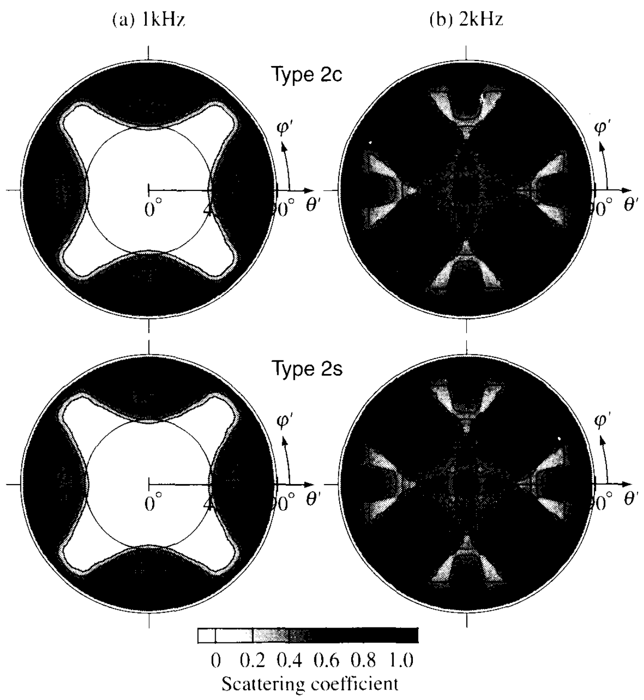

Fig. 11 Distribution of the directional scattering coefficients for Types 2c and 2s: (a) 1 kHz and (b) 2 kHz.

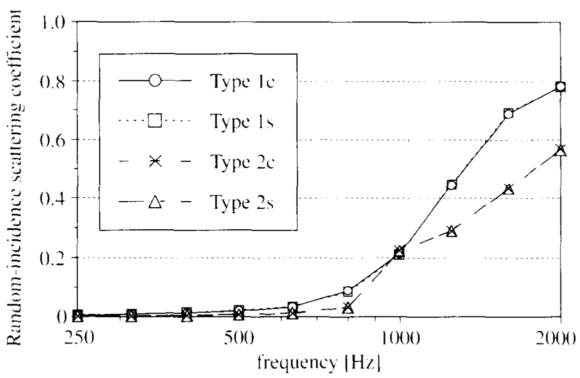

Fig. 12 Random-incidence scattering coefficients for two sets of circular and square samples.

Table 3 Four types of test samples. L is the period and h is the height.

	L (m)	h (m)	Number of periods
Type O	0.167	0.05	18
Type A	0.200	0.06	15
Type B	0.300	0.09	10
Type C	0.600	0.18	5

4.2. Number of Periods in a Sample

In room acoustic designing, periodic surfaces are often used for the purpose of acoustic diffusion, thus a wall with them is one of the typical samples for evaluating the scattering coefficients. However, special attention in the test is required regarding the number of periods in a sample, in order to evaluate the representative values. In this subsection, four types of samples with 1D sinusoidal periods as listed in Table 3, are tested with changing the number of periods, where the samples have the constant ratio of the height h to the period L as $h/L = 0.3$ (see Fig. 3).

Figure 13 shows the distribution of the directional scattering coefficients for Types A, B and C, on the two conditions that L/λ is constant. If the sample area is infinite, the results for the three types should perfectly agree with each other, however, the calculated values become slightly larger as the number of periods decreases. It is considered to be due to the edge diffraction from the samples of different sizes in the scale normalized by period.

Figure 14 shows the random-incidence values in relation to the ratio L/λ. It is seen that the line gradually converges with increasing the number of periods. Figure 15 shows the differences ϵ_{np} between the above results on the two conditions of number of periods. Here, ϵ_{np} is expressed by the following equation as defined in subsection 3.2:

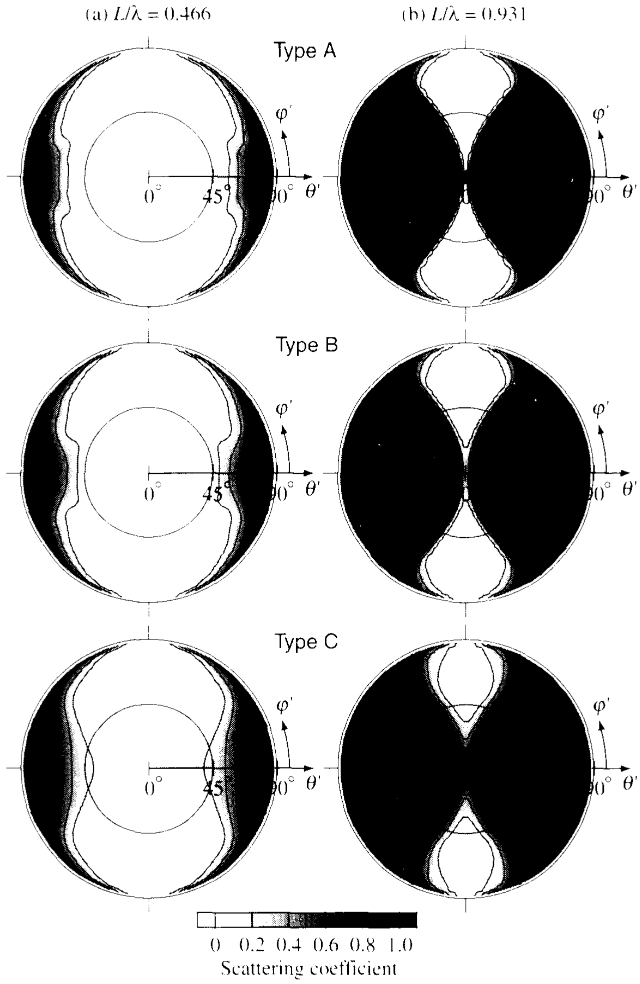

Fig. 13 Distribution of the directional scattering coefficients for Types A, B and C: (a) $L/\lambda = 0.466$ and (b) $L/\lambda = 0.931$.

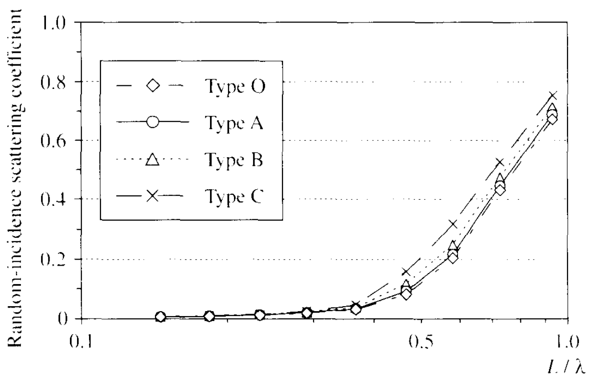

Fig. 14 Random-incidence scattering coefficients for four types of sinusoidal samples with different periods.

$$\epsilon_{np} = \frac{|\bar{s}_1 - \bar{s}_2|}{|N_{p,1} - N_{p,2}|}, \tag{7}$$

where N_p is the number of periods in a sample. While ϵ_{np} of Types B and C are varied depending on frequencies, it can

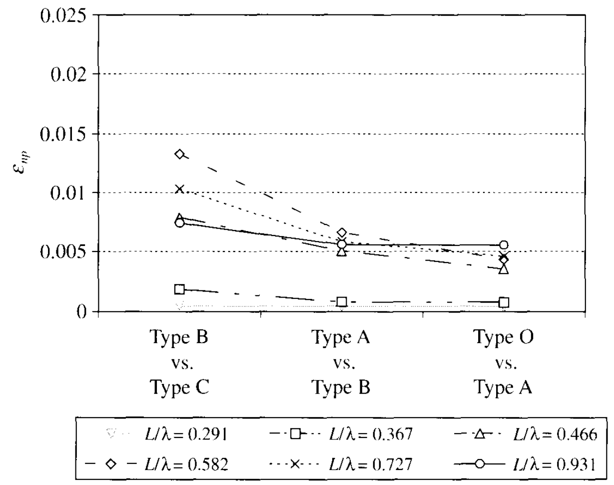

Fig. 15 Differences between the random-incidence values on the two conditions of number of periods. ϵ_{np} is defined as Eq. (7).

be seen that those for Types A and B are smaller than 0.01 independently of frequencies. Furthermore, those are almost smaller than 0.005 in the case for Types O and A. Consequently, 10–15 periods seem to be necessary for this kind of sinusoidal surfaces. This is roughly accord with the experimental result by Gomes *et al.* [12].

5. CORRESPONDENCE WITH THE SCATTERING COEFFICIENTS FOR AN INFINITE SURFACE

This section investigates the correspondence between the scattering coefficients for a test sample of finite size and for an infinite surface, which is mainly related with the influence of the edge diffraction. The circular sample with 1D sinusoidal periods with $L = 0.2$ m and $h = 0.06$ m (see Fig. 3) is analyzed as described above, while the infinite surface with the same periods is numerically analyzed with the Fourier series expansion [14].

Figure 16 shows the distribution of the directional scattering coefficients for the finite sample and for the infinite surface at 500 Hz, 1 and 2 kHz. The distributions for the finite sample have moderate gradation, which is considered to be due to the edge diffraction; and in contrast, clear patterns appear for the infinite surface although accompanying roughness due to the directional discretization. On the whole, correspondence between the distributions for the two surfaces can be seen to a certain extent.

Figure 17 shows the values of polar incidence angle dependence, averaged over azimuthal angles. As is seen in Fig. 16, a remarkable difference is seen at 1 kHz, and generally, the values for the finite are greater than those for the infinite. Naturally, the reason is that non-specularly reflected energy is overestimated due to the edge diffraction, and especially, this tendency becomes remarkable when the polar incidence angle is over 80 degrees.

Finally, Fig. 18 shows the random-incidence scattering coefficients at 1/12 octave-band center frequencies. Generally, the values for the finite sample and infinite surface relatively correspond with each other, although differences of about 0.1 occur because of the edge diffraction at middle frequencies. At high frequencies, the influence of the edge

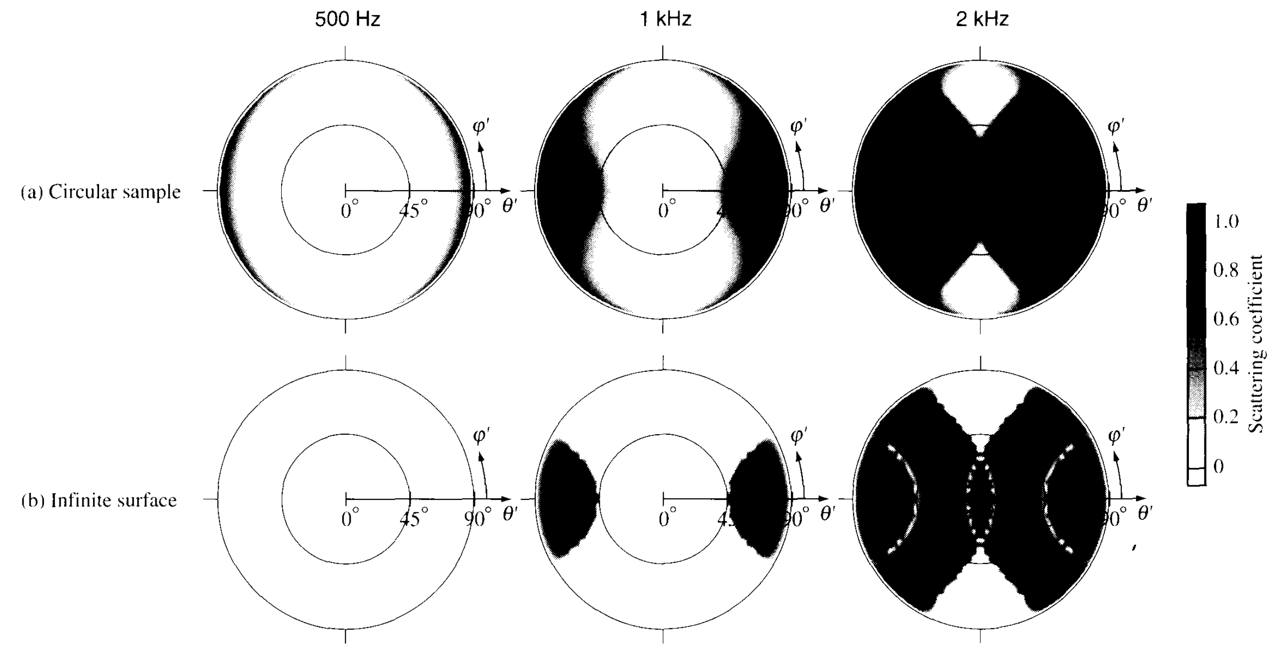

Fig. 16 Distribution of the directional scattering coefficients at 500 Hz, 1 kHz and 2 kHz, for (a) the circular sample and (b) the infinite surface.

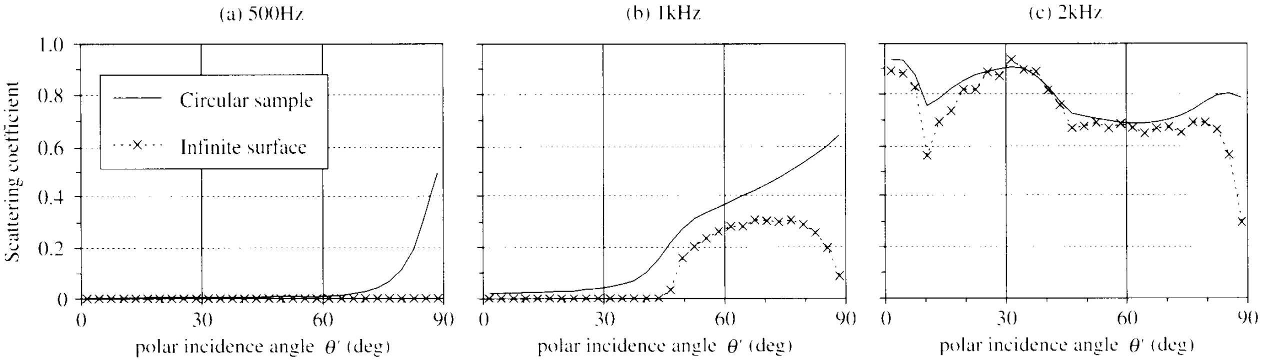

Fig. 17 Scattering coefficients of polar incidence angle dependence, for the circular sample and the infinite surface: (a) 500 Hz, (b) 1 kHz and (c) 2 kHz.

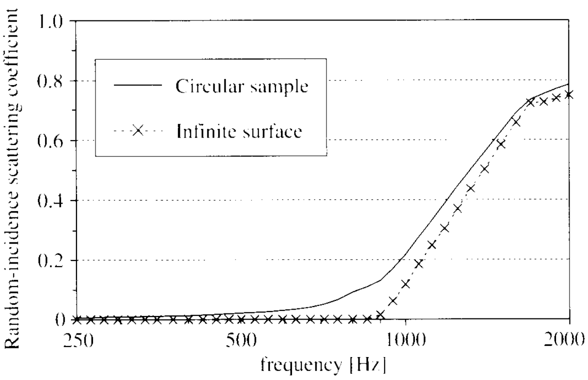

Fig. 18 Random-incidence scattering coefficients at 1/12 octave-band center frequencies for the circular sample and the infinite surface.

diffraction is so week that fairy good agreement is seen, and on the other hand, the effect of corrugated surfaces itself is very small at low frequencies.

6. CONCLUSIONS

As a practical method for evaluating the scattering coefficients of architectural surfaces, a numerical technique based on Mommertz's definition was developed with employing a 3-dimensional boundary element method. Numerical examination revealed the following findings for the setting of numerical parameters and the arrangement of test samples in the present method:

a) The distance from the center of a circular sample to receiving points is to be more than its diameter.
b) In directional discretization for incidence and reflection angles, the interval is to be roughly less than 5 degrees for the analysis up to 2 kHz.
c) For smooth or rough surfaces, the scattering coefficients at 1/6 octave-band center frequencies are sufficient to evaluate the values of 1/3 octave-bands, and the value at a 1/3 octave-band center frequency is almost equal to the average in the band.
d) As well as circular samples, square ones are also available for the present method based on Mommertz's definition.
e) For samples with periodic surfaces, the number of periods is at least to be 10, and more than 15 may be recommendable.

At last, in comparison between the scattering coefficients for a finite sample and for an infinite surface, general correspondence was confirmed in the random-incidence values, while it was clarified that some differences between them occur at middle frequencies due to the edge diffraction of the sample. Additionally, the influence of the edge diffraction appeared so obviously under grazing incidence that further investigation seems to be required.

REFERENCES

[1] K. Fujiwara and K. Masuda, "On the random reflection characteristics of a wall with periodical unevennes," *Proc. Spring Meet. Acoust. Soc. Jpn.*, pp. 581–582 (1989).

[2] D. Takahashi, "Development of optimum acoustic diffusers," *J. Acoust. Soc. Jpn. (E)*, **16**, 51–58 (1995).

[3] T. Yokota, "Study on effects of sound reflection plate and diffusers in rooms," *PhD Thesis, The University of Tokyo* (2001).

[4] AES-4id-2001, "AES information document for room acoustics and sound reinforcement systems — Characterization and measurement of surface scattering uniformity," *J. Audio Eng. Soc.*, **49**, 149–165 (2001).

[5] M. Vorländer and E. Mommertz, "Definition and measurement of random-incidence scattering coefficients," *Appl. Acoust.*, **60**, 187–199 (2000).

[6] ISO 17497-1: 2004, Acoustics — Sound-scattering properties of surfaces — Part 1: Measurement of the random-incidence scattering coefficient in a reverberation room (2004).

[7] J. Embrechts, "Practical aspects of the ISO procedure for measuring the scattering coefficient in a real-scale experiment," *Proc. Forum Acusticum Sevilla*, RBA-06-001-IP (2002).

[8] L. De Geetere and G. Vermeir, "Investigations on real-scale experiments for the measurement of the ISO scattering coefficient in the reverberation room," *Proc. Forum Acusticum Sevilla*, RBA-06-004-IP (2002).

[9] T. Sakuma and Y. Kosaka, "Comparison between scattering coefficients determined by specimen rotation and by directivity correlation," *Proc. Int. Symp. RADS 2004*, 056, 1–7 (2004).
[10] E. Mommertz, "Determination of scattering coefficients from the reflection directivity of architectural surfaces," *Appl. Acoust.*, **60**, 201–203 (2000).
[11] J. Embrechts, D. Archambeau and G. Stan, "Determination of the scattering coefficient of random rough diffusing surfaces for room acoustics applications," *Acta Acustica/Acustica*, **87**, 482–494 (2001).
[12] M. Gomes, M. Vorländer and S. Gerges, "Aspects of the sample geometry in the measurement of the random-incidence scattering coefficient," *Proc. Forum Acusticum Sevilla*, RBA-06-002-IP (2002).
[13] H. Kuttruff, *Room Acoustics*, 4th ed. (Spon Press, London, 2000), Chap. 2, pp. 31–58.
[14] S. Sakamoto, H. Mukai and H. Tachibana, "Numerical study on sound absorption characteristics of resonance-type brick/block walls," *J. Acoust. Soc. Jpn. (E)*, **21**, 9–15 (2000).